SIGNAL DESIGN AND PROCESSING TECHNIQUES FOR WSR-88D AMBIGUITY RESOLUTION

PART - I

National Severe Storms Laboratory Report
prepared by: M. Sachidananda
with contributions by: D.S. Zrnic and R.J. Doviak

July 1997

NOAA, National Severe Storms Laboratory
1313 Halley Circle, Norman, Oklahoma 73069

SIGNAL DESIGN AND PROCESSING TECHNIQUES FOR WSR-88D AMBIGUITY RESOLUTION

Part-1

Table of Contents

LIST OF SYMBOLS:

a_k, b_k, s_k, q_k	-	k^{th} spectral coefficient
c	-	speed of light
$C_{ab}(1)$	-	cross correlation of 1st and 2nd trip signals
C_k	-	complex modulation code [$C_k=\exp(j\phi_k)$]
e1, *e2*	-	complex time series of 1st and 2nd trips
E1	-	complex time series with 1st trip coherent and 2nd trip coded
E2	-	complex time series with 2nd trip coherent and 1st trip coded
E_i	-	complex time series samples
err( )	-	error in the parameter in brackets
f_d	-	Doppler frequency
f_a	-	Nyquist frequency
G_k	-	spectral coefficients (fitted to the Gaussian shape)
i, *k*, *n*, *m*	-	used as indices
j	-	$(-1)^{1/2}$
M	-	number of samples
n_w	-	notch filter width normalized by $2v_a$
nw	-	notch filter width in terms of number of spectral coefficients
N_k	-	noise power in the k^{th} coefficient
p1, *p2*	-	mean power of 1st and 2nd trips
pm1, *pm2* etc.	-	mean powers estimated from long PRT data
pw1, *pw2*	-	recovered 1st and 2nd trip powers (peak sorting algorithm)
P_k	-	power of the k^{th} spectral coefficient
r, r_τ	-	range
r_a	-	unambiguous range
$R_a(1)$, $R_b(1)$	-	autocorrelation of signals a and b
r(k)	-	random number array of length k
R(n)	-	autocorrelation for n PRT lag
R_p	-	residual power ratio (the ratio of power before notch filtering to the power after notch filtering, for the stronger signal)
R_o	-	overlapped power to total power ratio
S_k	-	power of the k^{th} spectral coefficient of the signal
S1, *S2*	-	spectrum of *E1* and *E2* [*S1*= DFT(*E1*)]
T	-	pulse repetition time
v_r	-	radial velocity
v_a	-	unambiguous velocity (short PRT)
v_{al}	-	unambiguous velocity (long PRT)
v_m	-	mean velocity
v1, *v2*	-	mean velocity of 1st and 2nd trips
vm1, *vm2*, etc.	-	mean velocities from long PRT data

vp1(i), vp2(i)	-	estimated velocity aliases of the1st and 2nd trips from long PRT data, i=1,2,3 & 4 (aliasing interval number)
w1, w2	-	spectrum width of 1st and 2nd trips
z	-	$\exp(j2\pi/M)$
$\wedge$	-	estimate
$\mathcal{P}$	-	probability
$\mathscr{E}$	-	expected value
τ	-	range time
ψ_k	-	switching phase sequence
ϕ_k	-	modulation phase sequence

ABBREVIATIONS:

SNR	-	Signal-to-Noise Ratio
PRT	-	Pulse Repetition Time
GCF	-	Ground Clutter Filter
DFT, IDFT	-	Discrete Fourier Transform, Inverse DFT
FFT	-	Fast Fourier Transform
S&S	-	Smoothing and Subtraction
$\pi/4$ code	-	{ 0 , $\pi/4$, 0, $\pi/4$, ... }
$\pi/2$ code	-	{ 0 , 0, $\pi/2$, $\pi/2$, ... }

SIGNAL DESIGN AND PROCESSING TECHNIQUES FOR WSR-88D AMBIGUITY RESOLUTION

PART - 1

1. INTRODUCTION

The Operational Support Facility (OSF) of the National Weather Service (NWS) has funded the National Severe Storms Laboratory (NSSL), the National Center for Atmospheric Research (NCAR), and the Forecast Systems Laboratory (FSL) to address the mitigation of range and velocity ambiguities in the WSR-88D system. This is the first part of the report on the ambiguity resolution in WSR-88D. It documents the work done at the NSSL in the first year of the project. Selected techniques that rely on spectral processing to sort out overlaid echoes are investigated, and the best candidate is selected for further scrutiny.

1.1. Range and velocity ambiguity

The range to scatterers is found by measuring the time delay between a transmitted pulse and its echo. If a transmitted pulse is part of an equi-spaced pulse train, the measured range is ambiguous because the echo signal could be due to any one of the pulses transmitted earlier (Doviak and Zrnic 1993). Therefore, the measured range, r, for a delay time, τ, is given by

$$r = (n\text{-}1)\, cT/2 + c\tau/2 \; ; \quad 0 \le \tau \le T$$

$$= (n\text{-}1)\, r_a + r_\tau \; , \tag{1.1}$$

where T is the pulse repetition time, c is the speed of light, r_a is the unambiguous range, and n is an integer or the trip number. Range ambiguity resolution is the determination of the trip number, n. Equation (1.1) implies that the echo measured at delay time τ could be due to any one of the pulses transmitted earlier, or in other words, the echo is due to scatterers located at any of the range cells corresponding to the time delay, $[(n\text{-}1)T+\tau]$. One simple method of determining the correct range is to choose T large enough to make $r_a=cT/2$ encompass ranges beyond which radar beam is about 16 km above ground so that no storms are intercepted, and $n=1$ can be assumed safely. However, this is not an acceptable solution because it severely curtails the velocity measurement capability of the radar.

The radial velocity of scatterers is obtained from the measurement of Doppler frequency,

f_d. The radial velocity of the scatterer is related to the Doppler frequency by

$$v_r = - \lambda f_d/2 \ , \tag{1.2}$$

where λ is the free-space wavelength. By convention, scatterers moving away from the radar have a positive velocity which produce negative Doppler shift. Because the echoes are discrete samples taken at intervals, T, the maximum Doppler frequency that can be unambiguously extracted from the sample sequence is given by

$$f_a = 1/(2T), \tag{1.3}$$

which is known as the Nyquist frequency. A fully coherent radar can recover Doppler frequencies within the interval $\pm f_a$. Any frequency outside this interval is seen by the processor as a measured Doppler frequency, f_d, within the aliasing interval such that

$$f_d - f_{da} = \pm 2 \, m \, f_a. \tag{1.4}$$

Here, f_{da} is the actual Doppler frequency. The integer, m, is the aliasing interval number. Therefore, the actual Doppler frequency is known only within an unknown integer, $\pm m$. Corresponding to the unambiguous frequency interval, $\pm f_a$, the unambiguous velocity interval is $\pm v_a$, where $v_a = \lambda/4T$. Since both v_a and r_a are functions of pulse repetition time, T, we can combine them to get

$$r_a \, v_a = c \, \lambda \, / \, 8. \tag{1.5}$$

Thus, if r_a is increased by increasing T, v_a decreases correspondingly. This is a fundamental limitation of a pulsed Doppler radar transmitting uniformly spaced pulses. However, the problem is overcome if means are found to determine the trip number, n, and the aliasing interval number, $\pm m$.

Discussions so far assume that the scatterers are located at only one of the several ambiguous locations corresponding to the delay, $[(n-1)T+\tau]$, and are moving with a certain radial velocity. In a pulsed Doppler weather radar, the situation is somewhat more complicated because the scatterers are precipitation particles that can be distributed quasi-continuously over a large area ($> 10^2$ km^2), and the dynamic range of the echo strength can be as large as 80 dB. Therefore, the echo sample can consist of echoes from more than one ambiguous range cell. If this is the case, the signals are said to be overlaid. Typical radial velocities encountered in storms can span a ± 50 m s^{-1} interval (Doviak and Zrnic 1993, p. 165, Fig. 7.4). The unambiguous range requirement for a 10 cm wavelength weather radar, such as WSR-88D, is about 460 km. Because of the curvature of the earth, the antenna beam would top most of the storms at about this range. If T is chosen to obtain r_a=460 km, the unambiguous velocity interval is too small to effectively de-alias velocities using data processing techniques. On the other hand, if T is chosen small enough to give at least ± 22 m s^{-1} unambiguous velocity, the echo signals from different range cells, corresponding to different trip numbers, n, may be overlaid.

In this case, one needs to separate the signals and then estimate their spectral parameters. Therefore, in the case of weather radar, ambiguity resolution must also include signal separation, in addition to the determination of trip number n and aliasing interval number, m.

In general, it may not be necessary to determine both m and n because if there is a technique to determine the trip number, n, one can choose a T short enough to make v_a encompass all the expected values of velocities so that m can be safely taken to be zero. Similarly, if there is a technique to find the aliasing interval, then T could be increased to yield a larger r_a. But echoes from subsequent pulses become less correlated as T increases, and therefore, spectral moment estimates deteriorate (Doviak and Zrnic 1993). At a 10 cm wavelength and a spectrum width of weather signals of 4 m s^{-1} (the median in severe storms), the decorrelation time (lag at which the correlation is $e^{-1/2}$) is about 2 ms, and the corresponding r_a = 300 km. Therefore, overlaid echoes are inevitable, and some kind of pulse to pulse coding (in time, frequency, phase, amplitude, polarization, etc.) or some a-priori information about the echoes, must be used to sort them.

Several methods which seek to ameliorate the problem of range and velocity ambiguity have been reported in the literature. Notable among them are (a) staggered PRT scheme (Zrnic and Mahapatra 1985) which can be considered as time coding, (b) random phase coding (Zrnic and Mahapatra 1985), (c) systematic phase coding (Sachidananda and Zrnic 1986), and (d) polarization coding (Doviak and Sirmans 1973). A radar that alternately transmits horizontally and vertically polarized waves can increase the unambiguous range by a factor of 2 (Zahrai and Zrnic 1993).

All these methods fall under the category of signal design and processing. There are other techniques developed to obtain aliasing interval information based on the continuity of velocity fields and/or knowledge of environmental winds. These techniques are implemented after fields of velocity are collected and can be classified as data field processing techniques.

The WSR-88D transmits pulses at two PRTs on sequential azimuthal scans or adjacent radials. The long PRT mode is for estimating the reflectivities over a large range, and the short PRT is for velocities over a smaller unambiguous range interval. In this scheme, unambiguous reflectivity information obtained in the long PRT scan is used to assign appropriate trip numbers, n, to signals in the short PRT scan. But in the case of overlaid echoes, only the stronger one is recovered in the WSR-88D signal processor. Further spectral processing could often recover the weaker echo as well. For example, the signal in the short PRT scan can be analyzed to locate peaks in the spectral domain and assign appropriate ranges to the corresponding velocities using the reflectivity information available from the long PRT scan. Such techniques fall in the category of spectral peak sorting, or simply peak sorting.

This report deals with signal design and processing techniques and examines methods that utilize a uniform PRT sequence with a sufficient number of samples for meaningful Fourier analysis (typically 64). Specifically, the following three are studied: (a) peak sorting, (b) random phase coding, and (c) systematic discrete phase coding. An in-depth simulation study has been carried out to evaluate their potential for possible implementation on the WSR-88D radar.

Except for peak sorting, the other two methods fall under the category of pulse to pulse coding or modulation. The main idea behind coding is to imprint some signature on the return signals corresponding to different transmitted pulses. These signatures are used to decode or separate the signals belonging to different trips. The methods (b) and (c) are different to the

extent that the code sequence is chosen differently, and an appropriate decoding scheme is evolved based on the properties of the modulated spectrum.

The report is organized in the following manner. In section 2, weather signal simulation procedure is discussed, along with the methodology for evaluating the algorithms developed for range and velocity ambiguity resolution in the presence of overlaid echoes. Then, in the subsequent three sections, several algorithms are discussed including the simulation results on the performance of the algorithms. In simulating the weather signal time series and in comparison of the methods of ambiguity resolution, the following assumptions are made:

a) the ground clutter is absent
b) the noise is absent
c) the window effect is absent
d) the spectra have a Gaussian shape
e) only the 1st and 2nd trip signals are present in the time series.

The decoding algorithms presented in this report are also developed with these assumptions. In practice, several of these effects, such as the window effect, the ground clutter, the noise, etc., are present and have to be accounted for in the algorithms. However, these are common to all, and would affect all the methods in some way or other in limiting their performance; hence they were neglected in evaluating the relative performance of the methods in order to identify the best one. These assumptions help bring out the basic capability of the methods which otherwise would be masked by some of these effects. The effect of the signal-to-noise ratio, the window effect, the ground clutter, and many more practical aspects of implementation of the algorithm on the WSR-88D are analyzed in Part 2 of this report where the selected method is scrutinized in much greater detail.

The WSR-88D in the present configuration can be operated in two different volume coverage patterns (vcp-11 and vcp-21), and in both, several preset PRT values are used which can be grouped as long PRT and short PRT. The long PRT is about 3 ms, and the short PRT is selected from a pre-defined set of values between 0.7 and 1 ms. The long PRT scan is called the surveillance scan (CS) and the short PRT scan is called the Doppler scan (CD). The volume coverage includes an azimuth scan of 360° at discrete elevation angles from 0.5° to 19.5° degrees. At the lowest two elevations (0.5° and 1.45°), two scans each (CS and CD) provide reflectivity to about 460 km and velocity to about 115 km, if there are no overlaid echoes. The number of samples available for spectral parameter estimation is about 16 to 17 samples in the long PRT scan and 44 to 66 samples in the short PRT scan, in the vcp-11 mode. In the vcp-21 mode, the number of samples is 28 for the CS scan and 75 to 111 for the CD scan.

In the scans at elevations 2° to 6.5°, the long and short PRT are used in alternate radials in each scan, called batch mode (B). The number of samples available for spectral parameter estimation is 6 to 10 with the long PRT, and 35 to 50 with the short PRT, in vcp-11. The corresponding numbers are 8 to 12 and 59 to 88 for vcp-21. Above 6.5° elevation, only the short PRT Doppler scan is used.

In the lower elevation scans (< 6.5°), the velocity recovery is hampered by overlaid echoes. The aim of this study is to evolve a solution to this problem. From the assumption (e) given above, it is obvious that the ambiguity resolution methods considered can, at best, extend

the range to only two trips. And if the unambiguous velocity is to be near 35 m s^{-1} , this extended range would be about 230 km. In the two lowest elevation scans, the unambiguous range requirement is about 460 km for the reflectivity; therefore, the long PRT scan must be retained. This leads us to the possibility of using the information from the long PRT scan data in ambiguity resolution algorithms applied to short PRT data. However, in the intermediate elevation scans (2° to 6.5°), the antenna beam tops a typical storm within the first two trips (about 230 km). Hence, there may be a possibility of replacing the batch scan with the Doppler scan, if the algorithm is able to extract all three spectral parameters of both the 1st and the 2nd trip echoes, with the required accuracy. Therefore, the methods of ambiguity resolution presented in this report are developed as stand-alone methods (not using long PRT data), whenever possible. But some methods are based on the availability of the long PRT data and cannot operate in a stand-alone mode. This is indicated in each algorithm.

2. SIMULATION STUDY.

2.1. Weather radar signal simulation.

In order to test the effectiveness of techniques for mitigating the range and Doppler ambiguities, it is desirable to make tests on overlaid radar signals. Comprehensive tests are necessary but are practical only on simulated radar signals because only with simulation can the actual individual signal parameters (i.e., the mean power, mean velocity, and spectrum width) be accurately known. The recovered parameters can be compared with the specified input parameters to determine the error in the estimates. However, the inferences drawn by this study can be meaningful only if the simulated weather spectra truly represent the radar signals from storms. Zrnic (1975) gives a procedure to simulate the weather signal on a digital computer using a random number generator available in most computers. The complex sample, E_i, in a time series can be expressed as a discrete Fourier series;

$$E_i = 1/M \sum_{k=0}^{M-1} P_k^{1/2} \exp(j\,\theta_k) \exp(j2\pi ki/M). \qquad (2.1)$$

Here, P_k is the exponentially distributed instantaneous power of the signal plus noise in the k^{th} spectral coefficient. The signal part is frequency dependent, and the noise part is white; θ_k is a uniformly distributed phase; and P_k and θ_k are statistically independent. With S_k as the signal power and N_k as the noise power, in the k^{th} coefficient P_k, the probability density of P_k can be written as

$$\mathcal{P}\{P_k\} = 1/(S_k+N_k) \exp[-P_k/(S_k+N_k)]. \qquad (2.2)$$

This is the basic equation used in the simulation of weather spectra. The steps include the generation of a Gaussian shaped S_k and adding a noise to get the desired signal-to-noise ratio (SNR). These coefficients are multiplied by the logarithm of a uniformly distributed random number (0 to 1) to get P_k. The phases, θ_k, are generated from the same uniform number generator but are independent.

This procedure was followed to generate weather signal spectra, and the inverse discrete Fourier transform (IDFT) was used to obtain the time series. To simulate the window effect, a very long time series is generated, and a short part, of length M, is taken and multiplied with appropriate weights. The window effect is not very critical in the evaluation of algorithms because it increases the spectrum width by a small amount. Simulating the window effect takes more computer time because long time series need to be generated. Therefore, for initial evaluations, the window effect was not included. The velocity aliasing is simulated by generating a time series without aliasing and then selecting alternate samples to simulate one-time aliases. Multiple aliasing is simulated by dropping n samples after each selected sample.

The program developed for time series simulation, "TSR1.M", has mean power, velocity, spectrum width, and number of samples, M, as the inputs. The output is a time series of complex samples (i.e., in-phase samples, I, and quadrature samples, Q) of length M. Three other

parameters, SNR, transmitter frequency, and PRT, are also included as inputs but are normally kept constant for most of the simulation. Although noise level is included in the time series simulation program, it is set to zero (SNR = infinity) in all the simulation studies presented in this report. Fig. 2.1 shows typical simulated in-phase and quadrature components of the time series and the spectrum. The parameters used for generating the signal are given in the figure.

The program, "TSR2.M", combines two time series, the 1st and the 2nd trip signals, into a single overlaid time series. The inputs to this program are the 1st and the 2nd trip parameters and the time series length, M. The program is made general so that any coding scheme can be implemented. The output time series has a coherent 1st trip, and the 2nd trip signal is coded. The options provided for the second trip coding are: (a) no coding, (b) $\pi/4$ and $\pi/2$ phase coding (Sachidananda and Zrnic 1986), (c) coding with a fixed predesigned random code, (d) phase code derived from $\phi_k=(n\pi k^2/M)$ with n as input (Chu 1972), and (e) internally generated random phase code every time it is called. In case (d), M is the time series length, and n is chosen as nearly prime to M (i.e., M is not divisible by n). This gives a phase code sequence, ϕ_k, which has cyclic autocorrelation zero for all lags except 0. If n is chosen such that M is an integer multiple of n, the code has a special property that its autocorrelation is non-zero and equal only for some discrete values of lags, and is zero for the rest. The $\pi/4$ code (Sachidananda and Zrnic 1986) is one such code which can be derived from this expression (i.e., $n/M=1/2$). The outputs of the program (TSR2.M) are a time series and the code sequence (except for option "a") which is required for processing. Thus, two overlaid signals of known spectral parameters can be obtained from this program. A sample spectrum of overlaid signal is shown in Fig. 2.2, as obtained from the simulation program.

In order to see how good our simulated signal is, we selected a nearly Gaussian-looking weather data from WSR-88D and generated a time series using the simulation program with the same spectral parameters. The two spectra are compared in Fig. 2.3, which shows a fairly good match.

2.2. The autocovariance algorithm.

When the echo signal is from a single range cell (i.e., no overlaid signal), the mean velocity is commonly estimated using the phase of the autocorrelation, $R(1)$, for one PRT lag. The autocorrelation $R(1)$ is estimated from the complex samples, $E_i = I_i + jQ_i$, using the formula,

$$\hat{R}(1) = (1/M) \sum_{i=0}^{M-1} E_i^* \, E_{i+1} \, , \tag{2.3}$$

and the mean velocity estimate is obtained from

$$\hat{v} = - (\lambda/4\pi T) \arg\{ \hat{R}(1) \} \, . \tag{2.4}$$

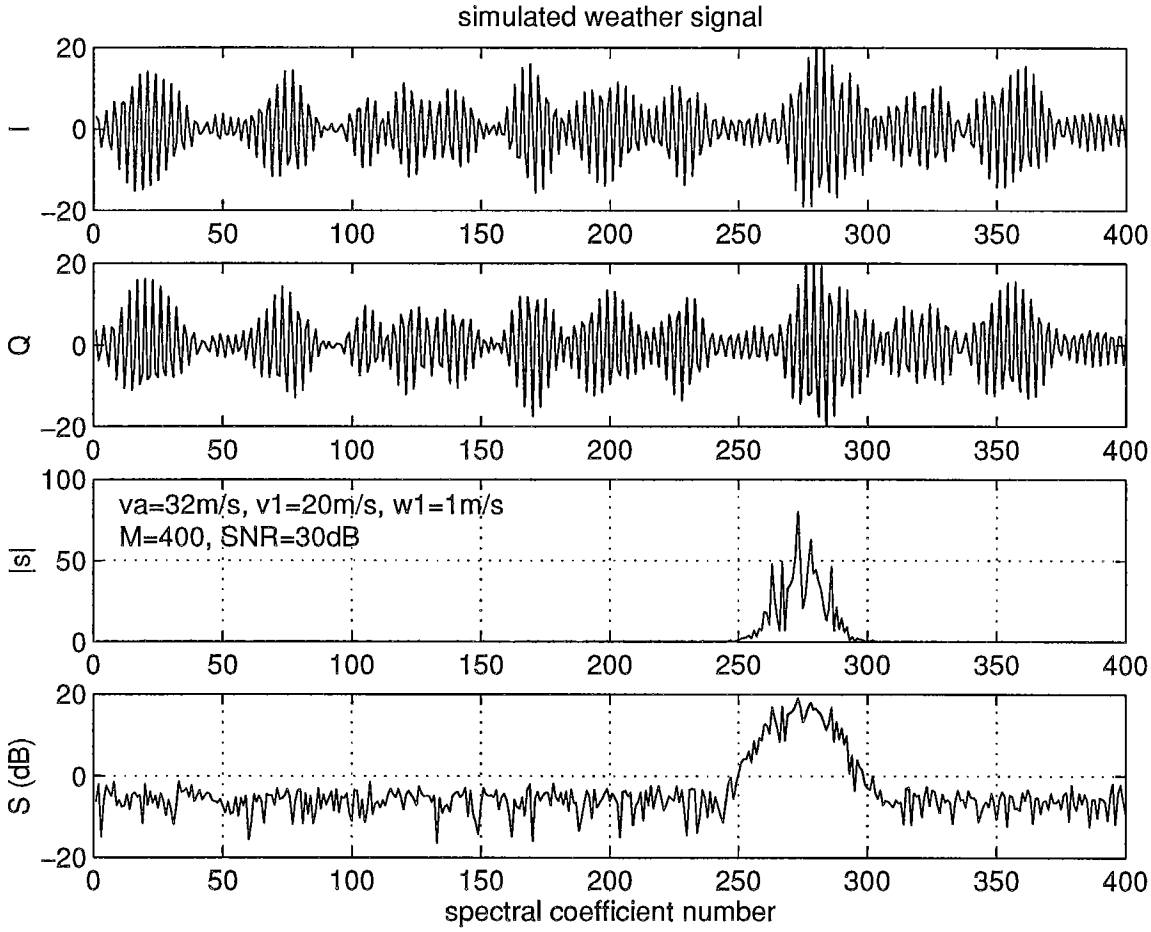

Fig. 2.1. A typical simulated weather signal; time series and frequency spectra. (a) the in-phase component, I, (b) the quadrature component, Q, (c) the magnitude spectrum, $|s|=\sqrt{(I^2+Q^2)}$, (the square root of the power spectrum on linear scale), (d) the power spectrum (dB scale).

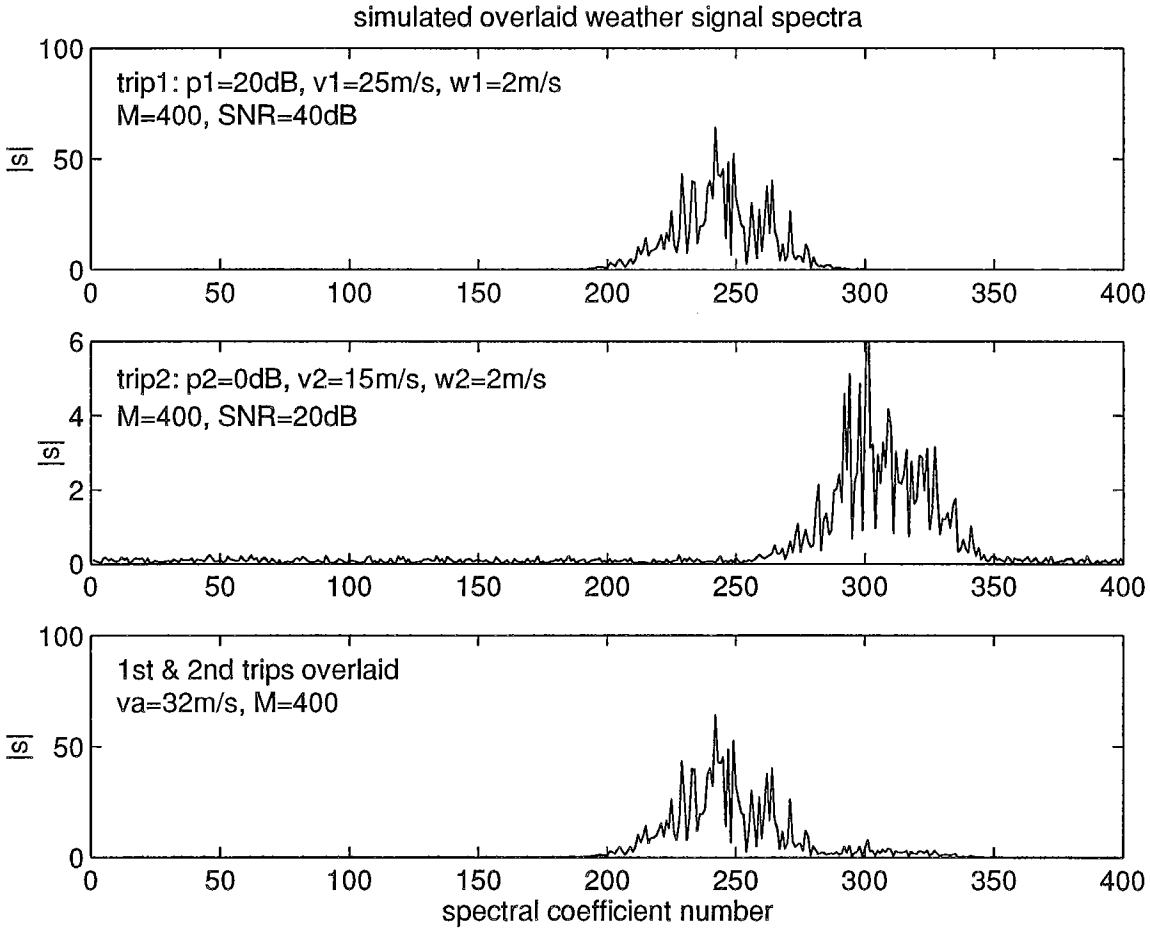

Fig. 2.2. A typical frequency spectra for simulated overlaid signals. (a) the 1st trip signal, (b) the 2nd trip signal, (c) the spectra of 1st and 2nd trip signals overlaid.

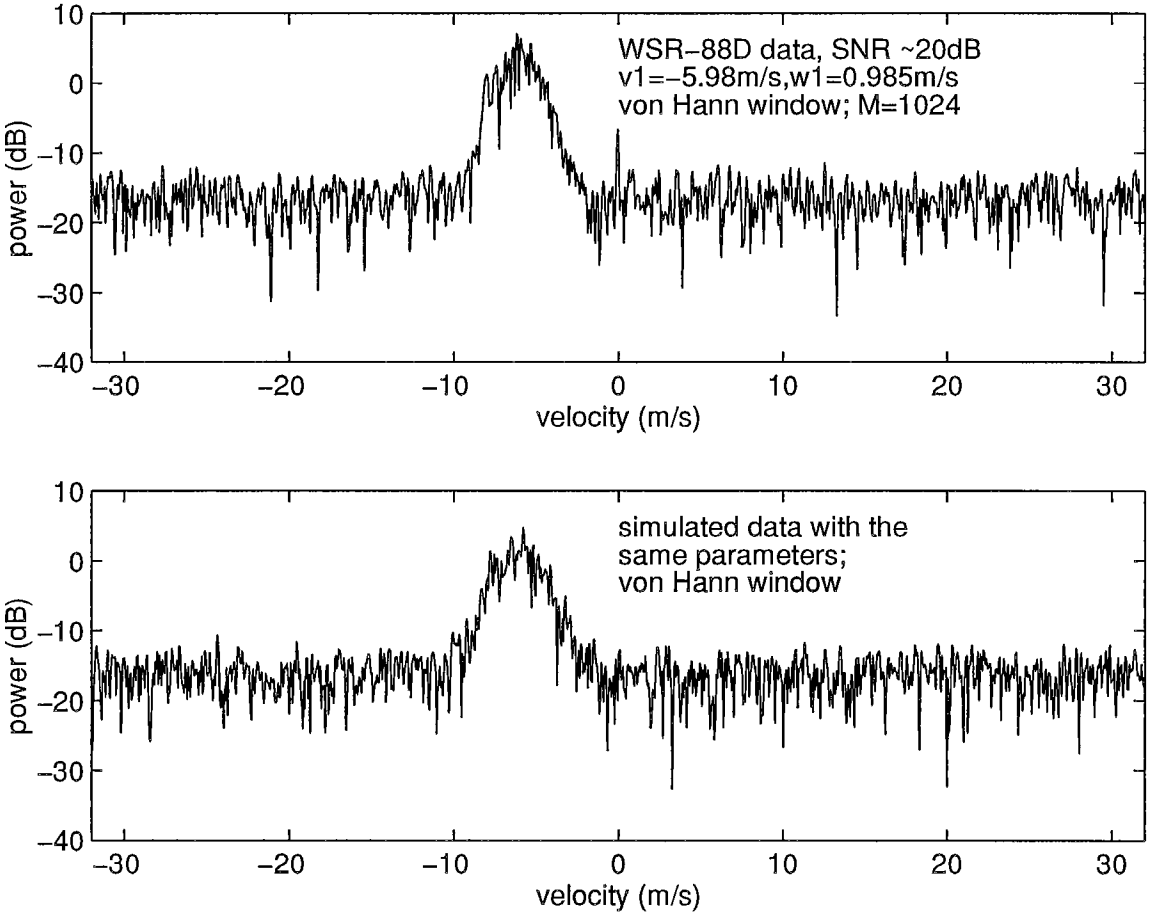

Fig. 2.3. A comparison of simulated weather spectrum with the spectrum of the data gathered from WSR-88D (WSR-88D data, courtesy: Frank Pratte, NOAA, FSL).

Here, the argument is in radians, and the velocity is in m s^{-1}. The symbol * represents a complex conjugate, and the symbol ^ denotes an estimate. This is commonly called autocovariance processing. The other two spectral parameters (i.e., mean power, p, and spectrum width, w) are estimated using the expressions given below. (see Doviak and Zrnic 1993 for details.)

$$\hat{p} = (1/M) \sum_{i=0}^{M-1} | E_i |^2 , \tag{2.5}$$

and

$$\hat{w} = (\lambda/2\pi T\sqrt{2}) \, | \ln (\hat{p} / |\hat{R}(1)|) |^{1/2} \, \mathrm{sgn}[\ln (\hat{p} / |\hat{R}(1)|)] . \tag{2.6}$$

In this study the computation of these three parameters is carried out in one program and is referred to as an autocovariance processor (program "pp.m").

When spectral coefficients are available and not the time series, the autocorrelation $R(1)$ can be computed from the spectral coefficients directly, without a transformation to the time domain, using the relation,

$$\hat{R}(1) = (1/M) \sum_{i=0}^{M-1} |s_i|^2 \exp(j2\pi i/M) . \tag{2.7}$$

In some of the algorithms discussed, there are situations where spectral coefficients are used for computing the autocorrelation (as well as the three spectral parameters) using the program "pps.m." This also is referred to as an autocovariance processor in this report, and no distinction is made between the two because both yield the same results.

2.3. Procedure for evaluation of algorithms.

The reflectivity, velocity, and the spectrum width are the three spectral parameters that need to be recovered for both the 1st and the 2nd trip echoes when they are overlaid. Of these three, velocity of the weaker signal is the most difficult to extract, and this is often the most important parameter of interest. Reflectivity, however, can be obtained from long PRT scan data, as is done in the WSR-88D radar. Spectrum width information is not used as often as the other two parameters. Thus, the recovery of velocity of the weaker signal decides the limit of usefulness of the algorithm. It is also observed during the course of the simulation study that the reflectivity of the weaker signal can be recovered over a larger dynamic range of overlaid signal power ratios than the velocity. Therefore, the error in the recovered velocity of the weaker signal is the parameter that is extracted in all the simulation runs. The errors in all other parameters (i.e., mean powers and widths) also are recorded over a large number of simulation runs. The commonly accepted error limits in the estimates are 1 dB for reflectivity, and 1 m s^{-1} for velocity and spectrum width. These limits are used in deciding the usefulness of the algorithms and in

comparing the different algorithms. It may be noted here that the reflectivity and the mean sample power are directly related but are not same. In all the simulations, the mean power is used and not the reflectivity, because the 1 dB accuracy required for the reflectivity estimate applies to the mean power estimate as well.

The error in the estimated velocity, as well as in the other parameters, depends on several factors, such as the spectrum width, noise level, window effect, number of samples in the time series, and the ability of the algorithm to recover the parameters. To separate these effects, and to evaluate the performance of the algorithm alone, first the number of samples, M, is taken to be large (M = 256) in simulation, and the noise level is set to zero. The window effect is also not included in the simulated time series. The variance of the velocity estimate, due to the spectrum width, cannot be removed because it is intrinsic to the signal, but for large M, it is within the specified limits. The signal parameters varied in the simulation study are the overlaid signal power ratio, *p1/p2*, the velocity difference, (*v1-v2*), and the spectrum widths of the two signals. For each set of parameters, several signal realizations were used to generate scattergrams of the error in the recovered velocity, *v2*, as a function of the variables of simulation. From these plots, limits of the algorithm were extracted. Later, to determine the practical limits of the algorithm, similar sets of simulations were run with M=64, which is about the maximum number of samples available in WSR-88D radar in the present working mode (vcp-11). In all simulations, the frequency is 3 GHz, and the PRT is 0.7812 ms. This choice gives an unambiguous range of 117.2 km and a Nyquist velocity of 32 m s^{-1}. In the presented data, the spectrum width can easily be normalized, with respect to the Nyquist velocity, to make inferences for a different Nyquist velocity.

Based on the results obtained on the performance of the algorithms (using M=64), a comparison was made to select a most promising method to recover the velocity of the weaker signal.

2.4. Programs.

The software, MATLAB, has been used for all the simulation work. The software was selected for its compact programs and matrix manipulation capabilities. Several signal processing functions are also available in the package which is very convenient for simulation work. Efficient 2-D as well as 3-D plot routines are also handy in graphical presentation of the results.

The programs developed for the simulation study of the algorithms are listed below with a brief explanation. Only important ones are listed; a large number of programs for generating the data and graphics are not included.

Simulation and decoding programs.

1. tsr1.m	Generates a simulated time series with the specified parameters, mean power, mean velocity, spectrum width, frequency, PRT, number of samples, and SNR.
2. tsr2.m	Generates overlaid signal time series. 1st and 2nd trip parameters and the coding to be specified.

3.	pp.m	Autocovariance algorithm. Outputs power, velocity, and spectrum width, with time series as input.
4.	pps.m	Equivalent of autocovariance algorithm with spectra as input.
5.	mfltr.m	Smoothing or running average filter. Filters an input sequence with a specified filter length.
6.	spc.m	Peak sorting algorithm.
7.	rndm.m	Decoding algorithm for random phase coded signal.
8.	piby2.m	Decoding algorithm for $\pi/2$ phase coded signal.
9.	piby4.m	Decoding algorithm for $\pi/4$ phase coded signal.
10.	msdz.m	Decoding algorithm for a systematic code based on $\exp(jn\pi k^2/M)$.
11.	testspc.m	Program to test the peak sorting algorithm.
12.	testrndm.m	Program to test the random phase code algorithm.
13.	testms2.m	Program to test the $\pi/2$ phase code algorithm.
14.	testmsdz.m	Test program for msdz.m
15.	testms4.m	Test program for the $\pi/4$ phase code algorithm.
16.	coder.m	Program used for optimizing the random code sequence.
17.	pps2.m	Autocorrelation processor for lag 2 computed in the spectral domain.

3. PEAK SORTING METHOD

3.1. Introduction.

This method requires a processor capable of the necessary computations in real time. Since no coding is employed at the transmitting stage, one has to depend on the available information about the signals to determine the mean velocities of the overlaid signals. The WSR-88D radar in the present configuration has a long PRT scan and a short PRT scan. The long PRT scan gives unambiguous reflectivity data over a 460 km range. This information can be used to assign the correct ranges to the estimated velocities of signals overlaid in the short PRT scan. That is, a comparison of powers associated with distinct spectral peaks, observed in the short PRT scan, with the powers from the long PRT scan, at ranges corresponding to τ and $(\tau+T)$ of the short PRT, is made to assign the velocity to proper ranges.

An assumption made in developing this algorithm is that the spectra have a Gaussian shape, which is an approximation for weather spectra. To recover spectral peaks with reasonable accuracy from a signal spectrum having considerable variance in each of its spectral coefficients, it is necessary to smooth the spectrum. However, smoothing the spectrum also smoothes the peaks and increases the width. The smoothing filter parameters have to be optimally chosen such that true peaks are not lost in the process of filtering and false peaks are kept to a minimum. The developed algorithm essentially locates and sorts the peaks in the spectral domain and assigns appropriate ranges to these velocities based on the data available from the long PRT scan. We assume that only 1st and 2nd trip signals are present in the spectra in developing the algorithm. It can easily be extended to a three or four trip signal overlay within certain restrictions.

3.2. Conceptual development.

The basic idea behind the development of this algorithm is that if two weather signals having Gaussian shaped spectra are present in a time series, these two peaks can often be identified in the spectral domain by a human observer, provided they are distinct. When the two spectra overlap, peaks may not be distinguishable. But based on the a-priori information available from the long PRT scan (i.e., aliased velocities can be computed from long PRT data), a decision can be made to assign the same velocity to both signals. Of course, there is an amount of error in this assignment when the velocities are close but not the same. How close the velocities can be before they merge into a single spectrum depends on the relative power levels of the two signals.

The first task, in developing the algorithm, is to locate the peaks of the spectrum. While a human observer can often locate the peaks by observing the shape of the spectrum, automatic recognition needs a computational procedure to locate the peaks. To avoid the computer selecting a local peak (associated with statistical fluctuations) rather than the global peak (associated with peaks of assumed unimodal spectra), it is necessary to first smooth the spectrum so that random fluctuations are reduced. Based upon extensive experimentation, a weighted running average filter applied to the magnitude of spectral coefficients is chosen as the smoothing filter. Note that the smoothing process preserves the power in the spectrum only approximately, and hence, the spectrum may not give a correct mean power estimate after smoothing. However, this is not a

problem since the reflectivity data is obtained from the long PRT scan, and it is sufficient to have approximate power estimates to identify the ranges. More important criteria would be the selection of the smoothing filter width and the weights. The performance of the algorithm is dependent on these parameters to a large extent. An ideal choice would have matched Gaussian shaped weights for the filter. Although spectrum width is estimated in the long PRT scan and can be used to obtain matched filter coefficients, here we have adopted an approach which does not make use of the width information. The main reason is that signals with different widths are involved. For practical implementation, it is convenient to have a fixed width and weights for the filter, although it may not be the best in all cases. Another advantage of a fixed filter width is that its effect on the power and spectrum shape can be evaluated and compensated, if required. A near optimum filter of fixed width and shape can be obtained by an experiment on simulated weather signals with a median width of 4 m s^{-1}. The optimum filter parameters (i.e., number of coefficients and weights) are functions of the time series length, M, and the unambiguous velocity or the PRT. The requirement of smoothing is such that it should remove random perturbations while retaining the shape and distinct global peaks in the spectrum.

After smoothing, first the largest peak of the spectrum is located and several coefficients on both sides of the peak are selected such that the magnitude of the coefficients at the ends is approximately 0.8 times the peak value. Then a Gaussian shape is fitted (i.e., least squares fit) to these coefficients. Thus, the peak of the fitted Gaussian curve gives the mean velocity of the strongest of the signals. To find the next peak, the Gaussian fitted spectrum is subtracted from the original spectrum before the second peak is located. The subtraction significantly enhances the probability of locating the peak of the second signal. This process is repeated further to locate third and fourth peaks. If the long PRT scan indicates significant power returns from more than two trips, the velocities of these also might be recovered. But the reason for locating more than two peaks is for more reliable recovery of the velocity data of the first two trips and not for recovering third and fourth trip velocities. Also the largest powers are not necessarily associated with 1st and 2nd trip echoes. One or both could be from 3rd and 4th trip. The long PRT data is used for assigning the correct trip numbers. Of the three or four peaks recovered, only two with the largest powers associated with them are selected. Note that when the peaks are sorted in decreasing order, the associated powers are not necessarily in the decreasing order because power takes into account the width, but the peak does not. If the peak is spurious with large amplitude and narrow width, the power associated with it will be small and hence, will be eliminated by the algorithm.

A measure of the spectrum width is also obtained from the fitted Gaussian shape. It should be noted that the width parameter does not directly correspond to the spectrum width of the original signal because of smoothing. Alternatively, spectrum width can be computed from the long PRT data, and this procedure is adopted in the algorithm.

A point to note here is that the magnitude spectrum is used for processing, and the curve fitting is done with a Gaussian shape function, $[\exp(-|v-v_m|^2/2w^2)]^{1/2}$. However, the spectral shape of the signal may not match the Gaussian shape because of the smoothing filter which changes the shape of the spectra to some extent. Therefore, this is another reason for mismatch in the shape in addition to the variability of the shape of weather spectra. The choice of processing in the magnitude domain was based on the results obtained (not given here) with three different options: power spectra, magnitude spectra, and square root of magnitude spectra. For a mean